

Nonmetallic transport property of the Si(111)7×7 surface

T. Tanikawa, K. Yoo,* I. Matsuda, and S. Hasegawa†

Department of Physics, School of Science, The University of Tokyo, 7-3-1 Hongo, Bunkyo-ku, Tokyo 113-0033, Japan

Y. Hasegawa

Institute for Solid State Physics, The University of Tokyo, Kashiwa, Chiba 277-8581, Japan

(Received 26 May 2003; revised manuscript received 15 July 2003; published 18 September 2003)

The electrical surface transport property of the Si(111)7×7 reconstruction associated with the space-charge region and with the surface-state band was studied as a function of temperature (80–400 K) with the micro-four-point probes in ultrahigh vacuum. Electrical conductance near the surface increases with increasing temperature, which is opposite to that of the bulk Si crystal in the temperature range investigated. This can be explained by the hopping conduction of mobile carriers jumping between empty sites of donor-impurities underneath the Si(111)7×7 surface with a small surface-state contribution. The thermally activated hopping conduction through the surface-states is also proposed in terms of localized nature of the adatom dangling bonds.

DOI: 10.1103/PhysRevB.68.113303

PACS number(s): 73.25.+i, 68.35.Rh, 68.35.Bs

Generally, modern quantum solid theory explains well the electronic transport property of a macroscopic material in terms of an electronic band structure and a critical role of density of states near E_F with a few exceptions such as strongly correlated electronic materials.¹ However, this correlation is still not clear in reduced dimension of solids.² Surfaces, interfaces, and ultrathin-overlayer-metal films are special class of low-dimensional materials since their physical properties are markedly different from their three-dimensional (3D) counterparts. Their well-defined electronic band structures data are already abundant from angle resolved photoemission spectroscopy (ARPES) experiments and first principles calculations.^{3,4} The time is certainly ripe for ultrasmall-scale electrical transport measurements.⁵ Surely, the direct measurements of electrical conductivity in reduced dimensionality such as surfaces and interfaces are needed for a better understanding of a correlation between the electronic surface band structures and the transport properties. Then it may be possible to classify such two-dimensional systems as new materials without lack of information, that is, an electrical transport property.

The Si(111)7×7 surface is an interesting prototype for surface transport studies since it is known to have “metallic surface-states” from ARPES studies and theoretical band calculations.^{6–8} In a brief description of the well-known Takayanagi model the surface consists of 1 corner atom, 6 rest atoms and 12 adatoms per unit cell, which means each atom has a dangling bond (DB) with one electron, total 19 electrons.⁹ It turns out that the corner atom and the rest atoms are completely filled (14 electrons) with energy levels from 1 to 2 eV below the Fermi energy, leaving five electrons for the adatom dangling bonds (ADB’s). Theoretical calculations have predicted that only two electrons per unit cell or 3.2×10^{13} e/cm² are responsible for the metallic behavior of the surface.⁷ Recent low temperature ARPES data⁸ show a very sharp band peak near E_F that is related to the ADB’s and the formation of a well-defined two-dimensional electrical surface, which requires direct manifestation in the

point of the fundamental definition of a metal or conductivity decreasing with increasing temperature T by measuring the electrical transport property.

In spite of technical difficulties several groups have attempted to measure the electrical transport of the Si(111)7×7 through a surface-states band. Persson have deduced the temperature dependence of ac surface conductance from electron energy loss spectroscopy (EELS) data, which varies linearly with temperature. The surface conductance at room temperature (RT) was about 10^{-5} S/□.¹⁰ Hasegawa and Ino¹¹ monitored simultaneously the resistance of Si(111)7×7 and Si(111) $\sqrt{3} \times \sqrt{3}$ -Ag of the same Si substrate during deposition of a few monolayers silver at RT. The deduced surface-state conductance was about 10^{-6} S/□. Attempts with a scanning tunneling microscope (STM) have also been made and estimates range from 10^{-6} to 10^{-9} S/□ for Si(111)7×7 at RT.^{12,13} Recently, one of the authors reported the linear temperature dependence of surface conductance of Si(111)7×7 on silicon-on-insulator (SOI) wafer using macroscopic van der Pauw method and the measured value was about 10^{-4} S/□ at RT.¹⁴

Despite these tremendous efforts and significant contributions, the estimated surface-state conductance of the Si(111)7×7 at RT scatters from 10^{-4} to 10^{-9} S/□ mainly because of the indirect measurement methods and poor surface sensitivities, and consequently the direct conductivity measurements on a clean surface with both ultrahigh surface sensitivity and temperature dependence are required quantitatively and qualitatively. In this Brief Report we present a challenging work to solve the old paradigm of a “metallic surface-states” of the Si(111)7×7 reconstruction in the use of a novel tool, the micro-four-point probe (MFPP).⁵ The conductivity measurements with the reduced probe spacing of four-point probes up to 4 μm (we used 8 and 30 μm probes) showed a clear signature that isolates a surface from a bulk in semiconductors due to *magic* insulating layer.¹⁵ Since the surface space-charge layer (SCL) beneath the 7×7 reconstruction is known to be a depletion layer due to the Fermi-level pinning by the surface-state, the current

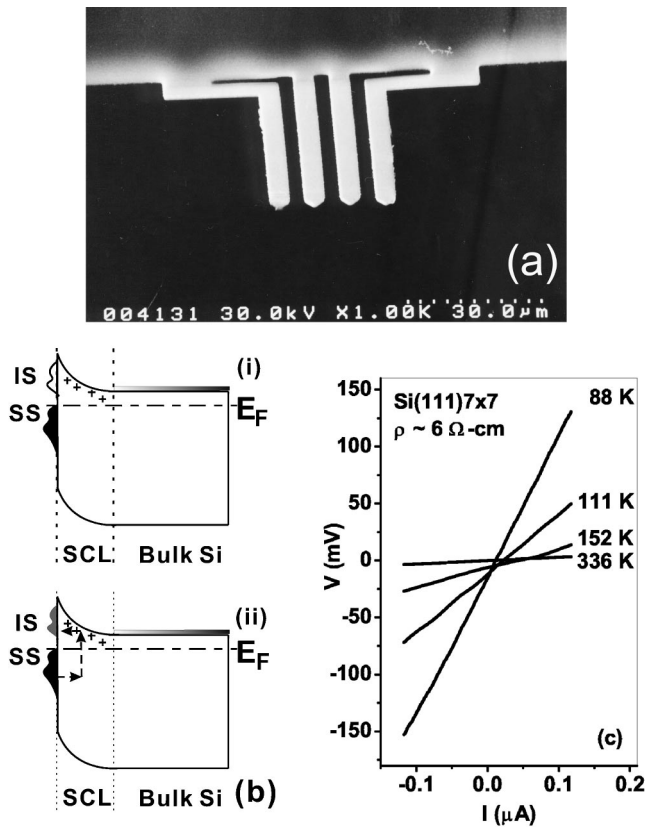


FIG. 1. (a) A typical micro-four-point probes tip with the spacing $10 \mu\text{m}$. (b) Simplified energy diagram near the surface: (i) before and (ii) after the electron injection (IS: Impurity states, SS: surface states) (not to scale). (c) The I - V characteristics on the $\text{Si}(111)7 \times 7$ surface at selected temperatures.

leakage into the bulk is small enough. Thus, the insulating depletion layer isolates the surface region from the bulk. The measured surface conductance of the $\text{Si}(111)7 \times 7$ shows a nonmetallic behavior with temperature, which means that the surface-state and the SCL conduction might be the main contribution due to the negligible bulk Si conduction contribution.

We used two phosphor-doped n -type $\text{Si}(111)$ wafers [$\rho_1 \sim 6 \Omega \text{cm}$ (sample I), $\rho_2 \sim 0.02 \Omega \text{cm}$ (sample II)] for conductivity measurements. Well-ordered 7×7 reconstructed surfaces were obtained by overnight degassing in ultrahigh vacuum (UHV) at 770 K, followed by repeated flashing up to 1370 K using a direct current heating method. Reflection-high-energy-electron diffraction (RHEED) patterns showed the clear formation of the $\text{Si}(111)7 \times 7$ reconstructions. Surface conductivity measurements were performed with the MFPP. The MFPP consists of four cantilevers as shown in Fig. 1(a), which are aligned in a row with each spacing of either 8 or $30 \mu\text{m}$ in our measurements. The MFPP can be controlled using a piezoactuator and four cantilevers with the spring constants of 1–10 N/m touch softly a sample surface, enabling nondestructive electrical conductivity measurements on a surface. In other word, the probes do not penetrate through the surface SCL. Electrical conductance can be measured by driving a dc current through outer two probes, while sensing voltage drop in inner two probes. A real time I - V curve can be recorded by a PC-based automated

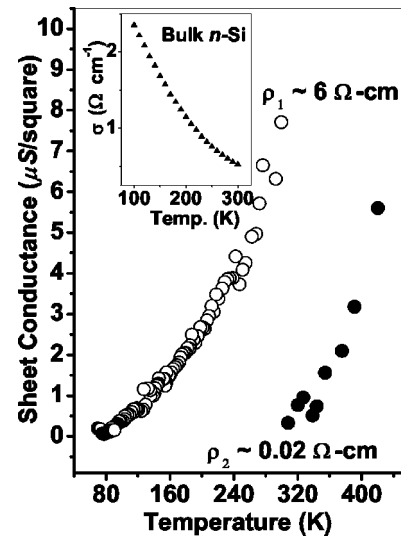


FIG. 2. Temperature-dependence of the surface conductance of the $\text{Si}(111)7 \times 7$. Both samples I and II show nonmetallic temperature coefficients. *Inset* shows the conductivity measurement of the $\text{Si}(111) \times 7$ with a macroscopic 4-probes.¹⁴

data acquisition with sampling up to 1600 data points.

We performed the surface conductance measurements on samples I and II. Figure 1(c) shows the I - V characteristic for low fields on sample I at selected temperatures. These nearly linear I - V curves show a new capability of MFPP for the electrical characterizations of semiconductors with ultrahigh surface sensitivity in UHV. It should be noticed here that the four-point probe method gives us correct resistances irrespective of Ohmic or non-Ohmic contacts at the probe contacts. Linear I - V curves are obtained even for nonmetallic samples, which is different from that in the case of (scanning) tunneling spectroscopy. The I - V slope which determines the resistances of $\text{Si}(111)7 \times 7$ surface becomes sharpen with decreasing temperature. The magnitude of the measured resistance R at about 300 K is about 38 k Ω and the converted conductivity is about $0.005 (\Omega^{-1}\text{cm}^{-1})$ that is well below the nominal wafer conductivity of about $0.17 (\Omega^{-1}\text{cm}^{-1})$. These imply that our MFPP measurements do not sense the component of bulk Si conductance but that of the surface and the subsurface of the $\text{Si}(111)7 \times 7$ due to the smaller probe spacing and the magic insulating SCL. Therefore, the sheet surface conductance, in the units of S/\square , can be described as follows, assuming a negligible bulk Si conduction contribution¹⁶ in our MFPP measurements:

$$\sigma_{exp.} = \sigma_{sc} + \sigma_{ss}, \quad (1)$$

where σ_{sc} and σ_{ss} are respectively the conduction through the SCL and through a surface-state band.

Figure 2 shows the temperature dependence of the sheet surface conductance of the $\text{Si}(111)7 \times 7$ on two Si samples of different resistivity. All data are extracted from the linear I - V curves. The sheet surface conductances of the $\text{Si}(111)7 \times 7$ in both samples increase with increasing temperature, which is opposite to that of the bulk Si crystal in this temperature range.¹⁷ It should be addressed in this point that at

the saturated temperature range (50~400 K) the total sheet conductance of the Si(111)7×7 measured by a macro four-point probe decreases linearly with increasing temperature.¹⁴ Actually, the dominant transport mechanism of a moderately doped bulk Si is phonon scattering. The change of the mobility leads the metallic temperature dependence under the constant carrier density.¹⁷ It clearly means that our MFPP results on the Si(111)7×7 involve a different electrical transport mechanism due to the isolation from the bulk Si layer band conduction.

We hereby propose that the involved electronic transport mechanism of the MFPP measured results (σ_{exp}) on the Si(111)7×7 surface is the combination of the hopping conduction (σ_{sc}) by a lateral space charge limited current (LSCLC) and the small contribution of the surface-states (σ_{ss}).¹⁸ Figure 1(b) shows a simplified energy band diagram before the electron injection (empty impurity states), and it will turn into a conduction channel (filled impurity states) after the electron injection.

This thermally activated hopping conduction of the SCL (σ_{sc}) can be explained as analogous to the well-known impurity conduction at very low temperature (freeze-out range). Most of free electrons in the freeze-out range are recaptured by the donor-impurities (for n-type) and weakly localized around the donor-impurities, and then the electron conduction by hopping (or tunneling) directly between the donor-impurities dominates over the free-electron band conduction.¹⁷ Likewise, free electrons of the SCL underneath the Si(111)7×7 surface are captured by the surface-states, leaving the empty donor-impurities inside a SCL without compensating charges. This is a depletion layer due to band bending. At low voltage and relatively high temperature electrons are injected from the electrode into the empty impurity states of the SCL beneath the Si(111)7×7 surface and the thermally activated electrons jumping (or tunneling) between the available empty donor-impurity sites mainly contribute to the conductivity. The free electrons in the bulk Si layer are prohibited to jump into the donor-sites due to the band bending and the no available empty sites. Otherwise, the band bending rule of $Q_{sc} + Q_{ss} = 0$ is violated, where Q_{sc} and Q_{ss} are the total charge per unit area in a SCL and in surface-states. This situation implies that the SCL layer is still insulating and the thermal activation of electrons are required for carrying a current. The remarkable decrease of the sheet conductance at RT and the nonmetallic temperature coefficient indicate obvious phenomena resulting from the band conduction to the hopping conduction in our measurements on the S(111)7×7 surface. It is due to the low density and low mobility of mobile carriers that are associated with a weak overlap of wave-function tails from neighboring impurities.

We will now discuss on the conduction through the “metallic surface-states” of the Si(111)7×7. The sheet surface conductance of the Si(111)7×7 at RT are about 5.8×10^{-6} S/□ (sample I) and about 4.5×10^{-7} S/□ (sample II) depending on the bulk doping levels. It means that our results are not simply the surface-state conduction of the Si(111)7×7 because the surface-state conduction should be intrinsic, irrespective of the bulk Si doping levels. Since the depletion width W ¹⁹ is about 350 nm in sample I and 35 nm in sample

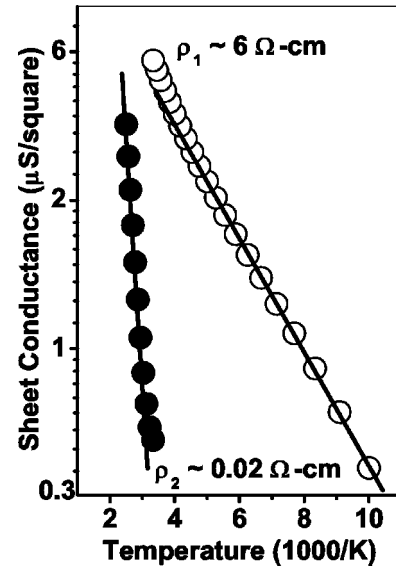


FIG. 3. The semilog plot of the surface conductance of the Si(111)7×7. Activation energies are 33.0 ± 0.4 meV below ~ 200 K in sample I and ~ 281 meV in sample II.

II at RT and closely related to the conductivity of the hopping channels, the sheet surface conductance is related to the depletion width of the SCL with the excess change of the surface-state channel conduction. Nonetheless, our results at RT are comparable with the range (from 10^{-4} to 10^{-9} S/□) of the sheet conductance of the other group’s results on surface and/or surface-state conduction of the Si(111)7×7.¹⁰⁻¹⁴

Figure 3 shows a semilog plot of the dependence of the sheet surface conductance (fitted data) on inverse temperature in the sample I and II. The sheet surface conductance in both samples decreases exponentially with increasing inverse temperature. The obtained activation energies from the equation $\sigma \sim \sigma_0 \exp[-E/k_b T]$ are 33.0 ± 0.4 meV below ~ 200 K in sample I and 281 meV above ~ 340 K in sample II. Both activation energies are much higher than that of the hopping conduction of the bulk Si (~ 2.0 meV) at very low temperature (lower than ~ 5 K).²⁰ This may be due to two possible reasons: the surface-states and the high temperature range. It has been predicted that the required activation energies for transferring an electron from an occupied adatom to a nearest empty adatom or a corner-ring at the Si(111)7×7 are ~ 80 meV and ~ 150 meV.²¹ This means that the conduction contribution of the ADB’s happens at relatively high temperatures. The reduction of the SCL conduction is also known to be large with increasing impurity concentration.²² As a consequence, the high activation energy at high temperature and in a high doped Si sample is expected. At large, such high activation energy of ~ 281 meV in the sample II may be a possible onset caused by the surface-state hopping conduction contribution. We feel that the electron injection into the SCL may also cause the high activation energy. Besides, the transport data interpretations in high temperature have been one of the main obstructions in explaining the electrical conductivity results quantitatively. More investigations are needed on the trans-

port mechanism of the surface-state conduction of the Si(111)7×7 since our results still contain the SCL conduction, but the direct surface-state conductivity measurements are close.²³

In summary, the electrical surface transport property on the Si(111)7×7 exhibits a nonmetallic conduction. This can be explained by the hopping of electrons between empty impurity sites underneath the surface and with a small

surface-state conduction. The hopping conduction through the ADB surface-states is proposed in terms of the localized nature of the adatom dangling bonds.

We would like to thank Professor F. Gray of Technical University of Denmark and Capres Company²⁴ for providing MFPP tips. This work was mainly supported by Grant-In-Aid from JSPS.

*Author to whom correspondence should be addressed. Electronic address: kjyoo@surface.phys.s.u-tokyo.ac.jp. Also at Institute for Solid State Physics, The University of Tokyo, Kashiwa, Chiba 277-8581, Japan.

[†]Electronic address: shuji@surface.phys.s.u-tokyo.ac.jp

¹P.W. Anderson, *Science* **235**, 1196 (1987).

²H.H. Weitering, X. Shi, P.D. Johnson, J. Chen, N.J. DiNardo, and K. Kempa, *Phys. Rev. Lett.* **78**, 1331 (1997); V. Ramachandran and R.M. Feenstra, *ibid.* **82**, 1000 (1999).

³C.B. Duke, *Chem. Rev. (Washington, D.C.)* **96**, 1237 (1996).

⁴K.D. Brommer, M. Needels, B.E. Larson, and J.D. Joannopoulos, *Phys. Rev. Lett.* **68**, 1355 (1992).

⁵S. Hasegawa and F. Grey, *Surf. Sci.* **500**, 84 (2002); I. Shiraki, F. Tanabe, R. Hobara, T. Nagao, and S. Hasegawa, *ibid.* **493**, 633 (2001); C.L. Petersen, F. Grey, I. Shiraki, and S. Hasegawa, *Appl. Phys. Lett.* **77**, 3782 (2000); I. Shiraki, T. Nagao, S. Hasegawa, C.L. Petersen, P. Boggild, T.M. Hansen, and F. Grey, *Surf. Rev. Lett.* **7**, 533 (2000); T. Tanikawa, I. Matsuda, R. Hobara, and S. Hasegawa, *e-J. Surf. Sci. Nanotech.* **1**, 60 (2003).

⁶R.I.G. Uhrberg, T. Kaurila, and Y.-C. Chao, *Phys. Rev. B* **58**, R1730 (1998).

⁷J. Ortega, F. Flores, and A.L. Yeyati, *Phys. Rev. B* **58**, 4584 (1998).

⁸R. Losio, K.N. Altmann, and F.J. Himpsel, *Phys. Rev. B* **61**, 10 845 (2000).

⁹K. Takayanagi, Y. Tanishiro, and S. Takahashi, *J. Vac. Sci. Technol. A* **3**, 1502 (1985).

¹⁰B.N.J. Persson, *Phys. Rev. B* **34**, 5916 (1986).

¹¹S. Hasegawa and S. Ino, *Phys. Rev. Lett.* **68**, 1192 (1992).

¹²Y. Hasegawa, I.-W. Lyo, and P. Avouris, *Surf. Sci.* **357-358**, 32 (1996).

¹³S. Heike, S. Watanabe, Y. Wada, and T. Hashizume, *Phys. Rev. Lett.* **81**, 890 (1998).

¹⁴K. Yoo and H.H. Weitering, *Phys. Rev. B* **65**, 115424 (2002).

¹⁵S. Hasegawa, I. Shiraki, T. Tanikawa, C. Petersen, T. Hansen, P. Boggild, and F. Grey, *J. Phys.: Condens. Matter* **14**, 8379 (2002); L. He and H. Yasunaga, *Jpn. J. Appl. Phys., Part 1* **24**, 928 (1985).

¹⁶Since the width of the SCL is not abrupt near the bulk Si in (n-type) low doped semiconductors, some population of carriers exist in the conduction band and may contribute in part to the conductivity at high temperature.

¹⁷S. M. Sze, *Physics of Semiconductor Devices*, 2nd ed. (Wiley, New York, 1981), p. 26 and p. 402; N. F. Mott and D. Gurney, *Electronic Process in Ionic Solids* (Oxford University Press, New York, 1940), p. 172; M.W. Klein, D.H. Dunlap, and G.G. Malliaras, *Phys. Rev. B* **64**, 195332 (2001).

¹⁸From the narrow surface-state bands of the ADB's it is quite reasonable to assume that the band conduction through the ADB's (if it is) might be small due to the low mobility of the carriers at the surface.

¹⁹ $W = \sqrt{2e\epsilon_0\epsilon_r v_s / Nq}$ ($\epsilon_0\epsilon_r$ is the dielectric constant, v_s the band bending (~ 0.15 eV at Si(111)7×7), and N the dopant level);¹⁷ see also F.J. Himpsel, G. Hollinger, and R.A. Pollak, *Phys. Rev. B* **28**, 7014 (1985).

²⁰B. I. Shklovskii and A. L. Efros, *Electronic Properties of Doped Semiconductors* (Springer-Verlag, New York, 1984).

²¹F. Flores, J. Ortega, and R. Perez, *Surf. Rev. Lett.* **6**, 411 (1999).

²²W. Mönch, *Semiconductor Surfaces and Interfaces*, 2nd ed. (Springer-Verlag, New York, 1995), p. 68; H. Lüth, *Surfaces and Interfaces of Solid Materials*, 3rd ed. (Springer-Verlag, New York, 1992), p. 361.

²³An independently driven low temperature four-tip scanning tunneling microscope (LT 4-tip STM) of our group appears to be a promising tool.

²⁴See Capres: www.capres.com